Journal of Catalysis **196,** 1–7 (2000)
doi:10.1006/jcat.2000.3010, available online at http://www.idealibrary.com on IDEAL®

Influence of the Reaction Atmosphere on the Characteristics and Performance of VPO Catalysts

R. Mallada,* S. Sajip,†,‡ C. J. Kiely,†,‡ M. Menéndez,* and J. Santamaría*,[1]

*Department of Chemical and Environmental Engineering, Faculty of Science, University of Zaragoza, 50009 Zaragoza, Spain; and †Department of Engineering and ‡Department of Chemistry, University of Liverpool, Liverpool, Merseyside, L69 38X, United Kingdom

Received December 1, 1999; revised June 26, 2000; accepted August 2, 2000

Butane-rich and oxygen-rich mixtures have been fed to a fixed bed reactor loaded with VPO catalyst used in the production of maleic anhydride. The experiments were designed in such a way that the evolution of the state of the catalyst surface and of the catalytic performance along the bed could be followed and related to each other. The results obtained indicate that a marked pattern of catalyst reduction exists in the reactor used under butane-rich conditions, leading to the appearance of V^{3+} phases. This causes a strong decrease in the selectivity to maleic anhydride. © 2000 Academic Press

INTRODUCTION

Notwithstanding the complex nature of VPO catalysts, it seems clear that one of the key variables controlling their performance in the oxidation of butane to maleic anhydride (MA) is the oxidation state of vanadium. Spent equilibrated catalysts typically exhibit a V valence state that is slightly higher than 4^+ (1), which suggests that V is mainly present on the catalyst surface as V^{4+}, with some V^{5+} centers. In fact, it has been recognized for a long time that active and selective catalysts need a moderately high oxidation state, involving the simultaneous presence of V^{4+} and V^{5+} centers on the catalyst surface (2). The use of both *ex situ* (e.g., XPS, ^{31}P NMR spin-echo mapping, and MAS (3)) and *in situ* techniques, such as laser Raman spectroscopy, (e.g., 4, 5) has confirmed the presence of phases characteristic of V^{4+} and V^{5+} under reaction conditions. In particular, the results of Soejarto *et al.* (5), who cycled the catalyst between oxidizing and reducing conditions, demonstrated the sensitivity of the VPO catalyst to the reaction atmosphere and provided evidence of the relatively fast and reversible transformation of $(VO)_2P_2O_7$ to various $VOPO_4$ polymorphs which are V^{5+} phases.

Recently, Rodemerck *et al.* (6) investigated the behavior of VPO catalysts with average degrees of oxidation ranging from 3.2 to 4.9. Catalysts with an average oxidation state of 3.7 or lower were not able to form MA, and only butene, butadiene, furan, CO, and CO_2 were observed. On the other hand, with VPO catalysts having a high degree of oxidation (average $V^{4.9+}$ consisting mainly of β-$VOPO_4$) only CO_2 was formed. However, it is interesting to note that these samples could be reduced under reaction conditions, and MA started to appear in the product stream when the average oxidation state of the catalyst fell below a value of $V^{+4.6}$. This was suggested to be due to the formation of a $(VO)_2P_2O_7$ phase on top of the β-$VOPO_4$ surface. For intermediate oxidation states these authors found an increase in the yield of MA with increasing valence state of V, (up to a maximum of +4.6). Thus, it seems that a limited amount of V^{5+} is necessary to obtain a high selectivity to MA, but excessive V oxidation leads to deep oxidation of the products to form predominantly CO and CO_2. Ait-Lachgar *et al.* (3) estimated that the optimal V^{5+}/V^{4+} ratio would be around 0.25, i.e., one V^{5+} site for every four V^{4+} sites.

Most laboratory studies with VPO catalysts involve fixed bed microreactors with very small sample sizes (often in the tens of milligrams range) in order to maintain homogeneity of the reaction atmosphere in contact with the catalyst. However, for higher values of W/F (catalyst to feed ratio) the variation of the reaction atmosphere is very significant: the oxygen/hydrocarbon ratio (where hydrocarbon includes not only butane, but also reaction products such as butenes, butadiene, and maleic anhydride) is highest at the reactor entrance and decreases throughout the bed as oxygen is progressively consumed. Thus, one can expect an increasingly reducing atmosphere from reactor inlet to exit. On the other hand, there are also non-hydrocarbon, oxygen-containing species (CO, CO_2, H_2O) which are generated as reaction products along the reactor, whose influence on the state of the catalyst surface is unknown. The butane conversion and MA selectivity measured at the reactor exit are the cumulative result of the reactions taking place over the different catalyst fractions in the bed. This work attempts to correlate the changes of the reaction atmosphere along the reactor with the physicochemical characteristics

[1] Corresponding author. Fax: +34976 762142. E-mail: iqcatal@posta.unizar.es.

0021-9517/00 $35.00

of the catalyst (oxidation state and specific phases present) and the observed catalytic performance.

EXPERIMENTAL

A schematic drawing of the reactor used is shown in Fig. 1. The reactor was a 10-mm-id stainless steel tube, with one inlet (number 1) and four 5-mm-id exits, marked 2 to 5 in the diagram. Four small fixed beds each containing 400 mg of VPO catalyst were packed close to each of the outlets as shown, separated by quartz wool plugs. The exit from each of the beds could be directed to an on-line gas chromatograph for analysis. In this way, the reaction atmosphere around each of the four catalyst samples could be known accurately.

The reaction took place at essentially atmospheric pressure and at a temperature of 450°C. The reactor was heated by means of a three-zone electrical furnace. A movable thermocouple inside an axial quartz thermowell (4 mm od) was used to monitor the temperature profile along the reactor. The maximum temperature deviations from the set point measured at any axial position were ±5°C. Mass flow controllers were used to feed the different gases to the reactor. During operation, the reactor was allowed to reach steady state with a specific inlet composition (exits 2 to 4 closed). Once a constant composition was achieved at exit 5, a small purge (less than 10% of the total flow) was drawn in sequence through each of the outlets, starting with exit number 4. The exit gases were analyzed by means of on-line gas chromatography, using three capillary columns in a single gas chromatograph equipped with TCD and FID detectors. The main products were butane, oxygen, maleic anhydride, CO, and CO_2. Carbon balance closures for the experiments reported in this work were better than ±5%. The exit gases were also analyzed for *n*-butene, *cis*- and *trans*-2-butene, butadiene, furan, and cracking products (in the C2 range). The cumulative selectivity to all of these products was always lower than 2%, and they are not included in the results given below.

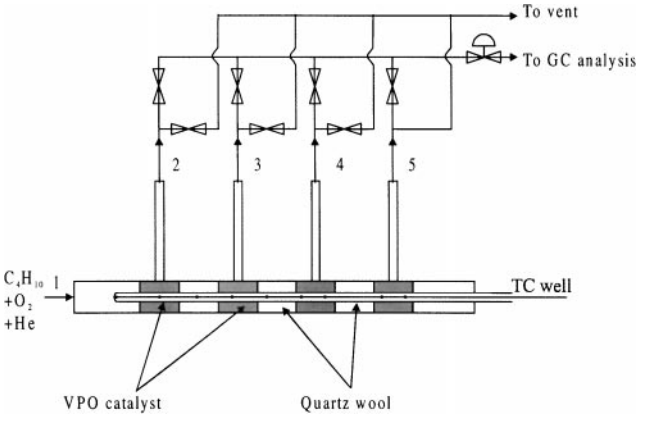

FIG. 1. Schematic diagram of the reactor setup.

The VPO catalyst used in this work was prepared by Du Pont within the framework of the European project BRPR-CT95-0046 and supplied as a powder, already in its active form. A BET surface area of 23 m^2/g for the fresh catalyst was determined from N_2 adsorption–desorption measurements (Pulse-Chemisorb 2700). The powder was pelletized, then crushed and sieved to a size of 160–320 μm, and then packed in the annular space between the quartz thermowell and the reactor wall in order to form the catalytic bed. The catalyst is believed to be similar, but not identical, to that used in commercial units. The reaction system used allowed us to take catalyst samples from the different reactor regions. To this end, steady-state operation was first established and gas samples were taken from the different outlets, as described above. The reactor was then cooled down to room temperature under a pure (99.999%) He flow and transferred to a He-swept glove chamber where each of the catalyst bed sections was discharged to a He-filled sealed glass tube for subsequent characterization.

X-ray diffraction (XRD) analysis was performed using a Rigaku/Max System difractometer (Ni-filtered Cu$K\alpha$ radiation, scan rate of 0.02 degrees/s). The evolution of the catalyst surface following step changes in the feed concentration was followed by diffuse reflectance (DRIFT) data, which were obtained using a Mattson Research Series spectrometer equipped with a Spectra-Tech environmental chamber and a liquid N_2-cooled MCT detector. High-resolution transmission electron microscopy (HRTEM) was performed on a JEOL 2000EX high-resolution electron microscope fitted with a LaB_6 source operating at 200 kV. Catalyst powders were ground gently using an agate mortar and pestle in the presence of ethanol. One or two drops of the resulting slurry was deposited onto a 3.05-mm holey carbon-coated copper mesh grid.

The evolution of the degree of catalyst reduction along the bed was calculated from the oxygen uptake measured with equilibrated catalyst in reoxidation experiments. To this end, after reaching steady state under a given set of operating conditions, catalyst samples were discharged as described above and transferred to a 6-mm-id quartz microreactor. Then, pulses of known volume containing O_2/N_2 mixtures were sent over the sample at the reoxidation temperature (450°C). Between pulses, the sample was kept under inert (99.999% He) atmosphere. An on-line quadrupole mass spectrometer (HIDEN HAL 2/201) was used to follow the evolution of the signals corresponding to mass 32 (oxygen) and 44 (CO_2). The latter was necessary because catalyst samples often contained adsorbed hydrocarbons and/or carbonaceous deposits, which under the conditions used in the experiments would be burnt to CO_2, contributing to the oxygen consumption observed. The total oxygen consumption was obtained from the difference between

the areas of the oxygen signals before and after the catalyst bed; the fraction of oxygen consumption contributed by catalyst reoxidation was then calculated after deduction of the amount corresponding to CO_2 formation (since CO formation was found to be negligible in the reoxidation experiments performed). Catalyst reoxidation was considered complete when oxygen consumption in the pulses sent over the catalyst could no longer be detected.

RESULTS AND DISCUSSION

Two different sets of experimental conditions were used, namely *oxidizing* (i.e., oxygen-rich) conditions under which a feed containing 2% butane, 20% oxygen, and 78% He was fed at the reactor inlet, and *reducing* (i.e., butane-rich) conditions with the time on stream where the feed contained 10% butane, 15% oxygen, and 75% He. The evolution along the reactor of the butane and oxygen conversions and of the selectivity to MA and CO_x ($CO + CO_2$) under both sets of conditions is given in Fig. 2. As could be expected, under reducing conditions the butane conversion rapidly reaches a nearly stable level of 22% as the oxygen conversion approaches 100%, whereas under oxidizing conditions there is an almost linear increase of butane conversion with reactor position. At any axial position along the reactor, butane conversions were between 2.9 and 3.7 times higher under oxidizing conditions, compared to reducing conditions. It must be noted, however, that despite the lower conversion, the catalyst used under reducing conditions is not less active; in fact the local reaction rate (measured as moles of butane converted per unit time and unit weight of catalyst) is higher under reducing conditions at the reactor entrance. The reaction rate quickly decreased in the remainder of the reactor due to oxygen depletion.

More remarkable is the selectivity trend displayed in Fig. 2: under oxidizing conditions the selectivity to MA was significantly higher throughout the bed. The oxidation of butane to MA is a typical example of a series-parallel oxidation network with a valuable intermediate product. In such cases, as the conversion increases the concentration of the intermediate product increases too, and deep oxidation of the intermediate species becomes more likely. Therefore, under otherwise comparable conditions, a tradeoff is usually found between conversion and selectivity, whereby increasing conversion implies sacrificing selectivity. The fact that oxidizing conditions lead to an increase in both the conversion and the selectivity compared to those under reducing conditions suggests that important changes have taken place on the catalyst surface.

Visual inspection of the catalyst discharged from different reactor positions revealed significant color differences: from light gray (entrance) to a somewhat darker gray (exit) under oxidizing conditions, and from light gray to an almost black color under reducing conditions. This suggests

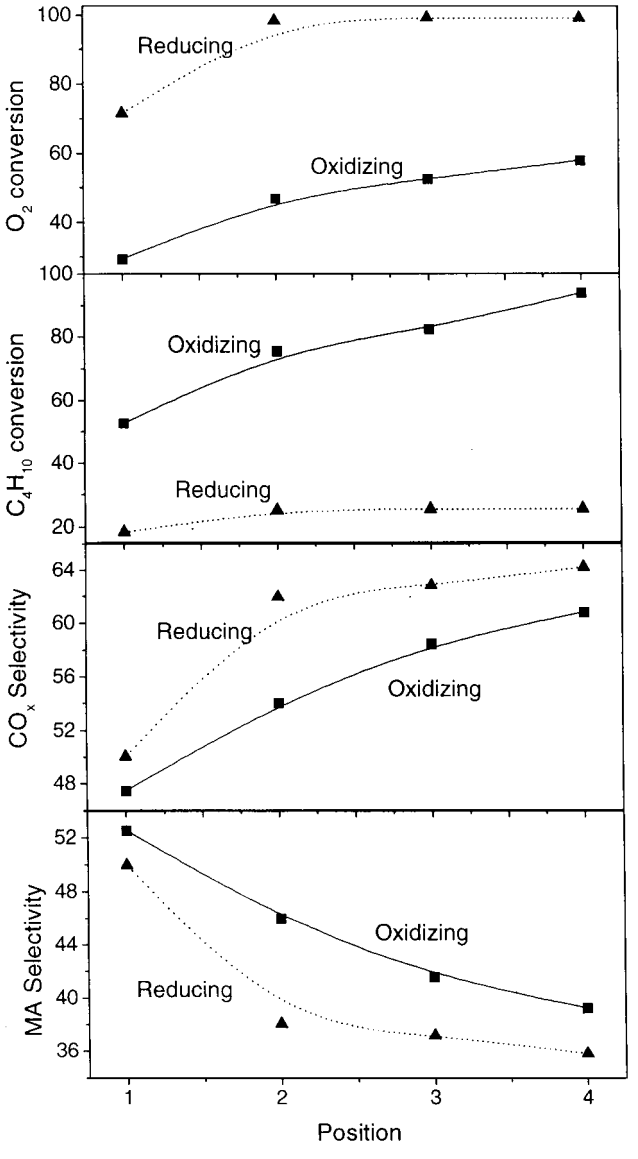

FIG. 2. Butane and oxygen conversions and selectivity to carbon oxides (CO_x) and MA as a function of reactor position, for oxidizing and reducing conditions.

that, while the state of the catalytic surface may be similar in both cases at the reactor entrance, reducing conditions would give a much more pronounced pattern of catalyst reduction along the bed. This was confirmed by the pulse reoxidation experiments carried out on the different catalyst samples (Fig. 3). The amount of oxygen consumed for reoxidation (after discounting CO_2 formation) increased along the bed in both cases, but the increase was much steeper for the catalyst used under reducing conditions. The figure also indicates that the catalyst in the first three positions of the reactor used under oxidizing conditions and the catalyst at the reactor entrance when used under reducing conditions had a similar and relatively high degree of oxidation, with very little oxygen uptake in the reoxidation experiments.

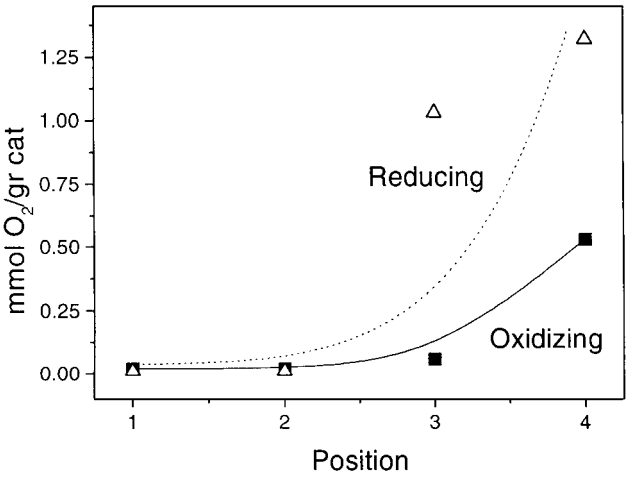

FIG. 3. Oxygen consumed during catalyst reoxidation as a function of reactor position for material exposed to oxidizing and reducing reaction conditions.

The amount of hydrocarbon material (carbonaceous deposits and/or adsorbed hydrocarbons) on the catalyst follows closely the pattern of catalyst reduction, as shown in Fig. 4 by the CO_2 produced during reoxidation. While the carbonaceous deposits reach concentrations above 2% by weight toward the exit of the reactor used under reducing conditions, there is little, if any, carbonaceous deposit on the first three positions of the reactor used under oxidizing conditions or at the reactor entrance under reducing conditions.

HRTEM characterization of all the samples used under oxidizing conditions showed that their appearance was very similar to that of the fresh catalyst. A typical example is shown in Fig. 5a, where it can be seen that the material is composed of crystalline micrometer scale $(VO)_2P_2O_7$

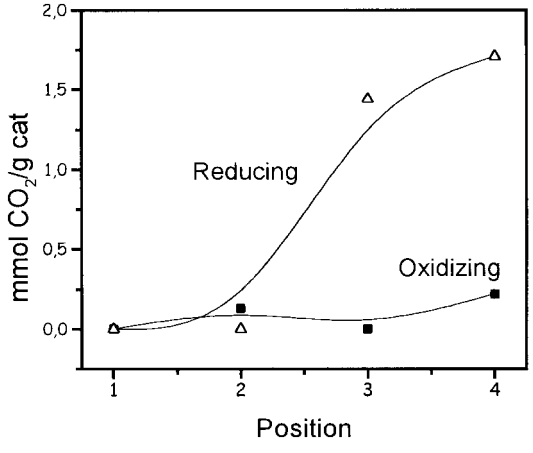

FIG. 4. Amount of CO_2 produced during the combustion of carbonaceous deposits on the catalyst surface during reoxidation experiments; the variation with reactor position is shown for oxygen-rich and butane-rich feed conditions.

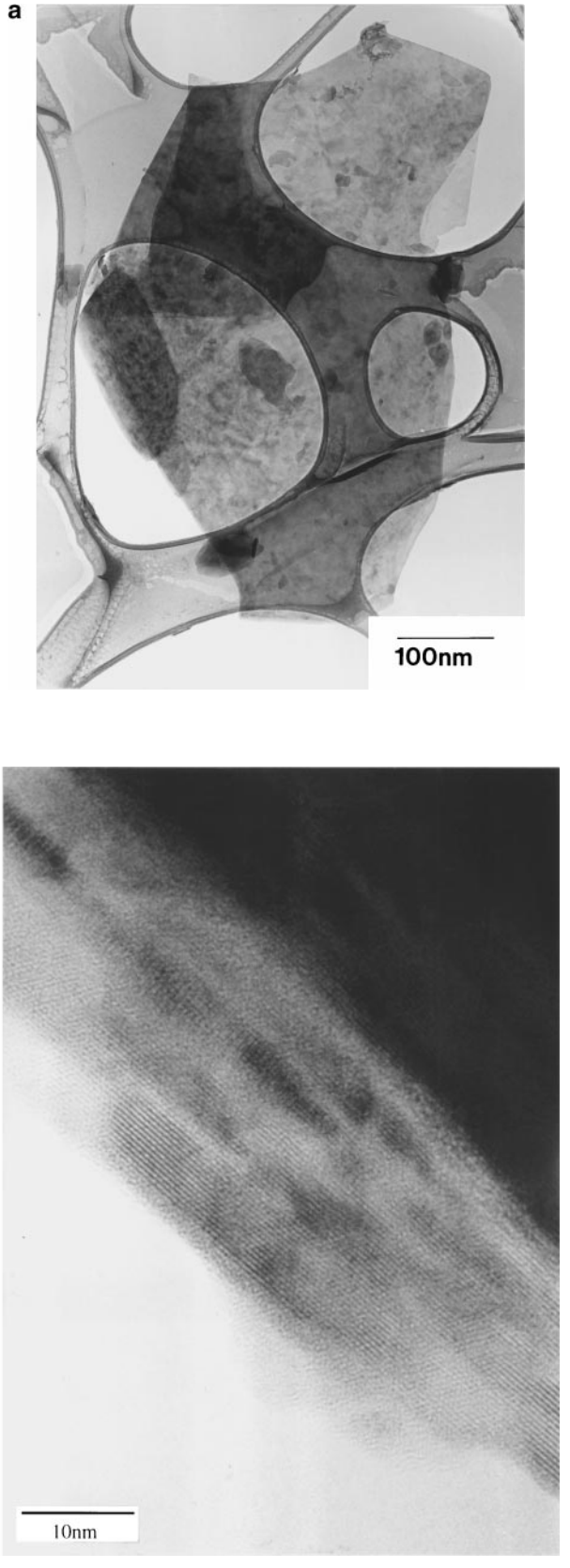

FIG. 5. Typical plan (a) and edge-on (b) views electron micrographs of a $(VO)_2P_2O_7$ platelet exposed to oxidizing reaction conditions.

platelets with a [100] surface normal. A very broad 200^{pyro} reflection, in XRD and electron diffraction, is indicative of occasional intercalated amorphous layers running parallel to the platelet surface (therefore effectively reducing the thickness of crystalline platelets). When viewed edge-on, these intercalated disordered layers can be seen as indicated in Fig. 5b. The platelets also always show a disordered surface layer; this could be as a result of rapid amorphization of surface $VOPO_4$ phases which are very prone to electron beam damage.

Specimens corresponding to positions 1 and 2 of the reactor used under reducing conditions look essentially identical to those shown in Fig. 5. However, the progressive introduction of planar shear type defects along two sets of $\{012\}^{pyro}$ planes that intersect the (100) pyro surface is evident as we move to positions 3 and 4 near to the reactor exit (as shown in Fig. 6). The effect is particularly marked at position 4. These are believed to be generated by the loss of lattice oxygen, which is the first step in the epitaxial transformation of $(VO)_2P_2O_7$ to VPO_4 (a V^{3+} phase). This topotactic transformation has recently been fully characterized (7) and maintains the following orientation relationship between the two crystal structures:

$$[100]\text{pyro}//[1\bar{1}0]\ VPO_4 \quad \text{and} \quad [001]\text{pyro}//[001]\ VPO_4.$$

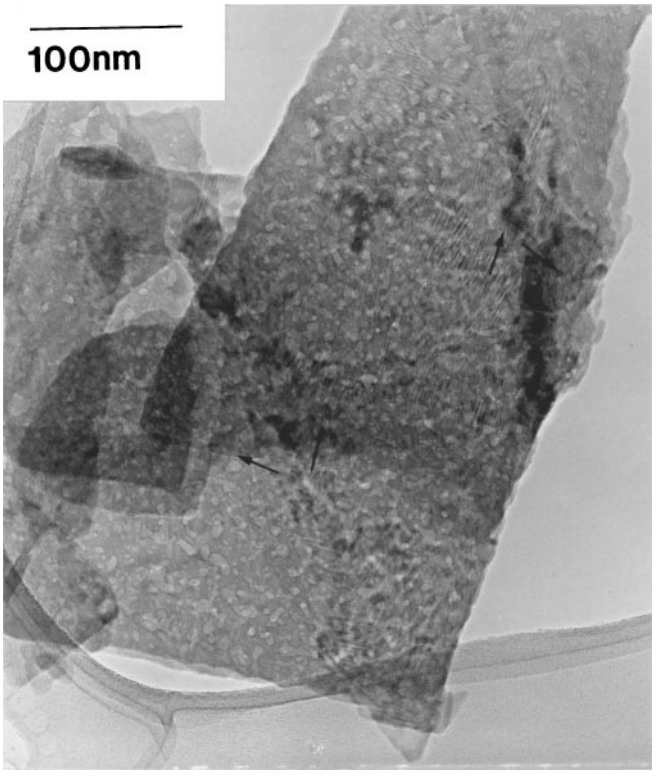

FIG. 6. Electron micrograph of a $(VO)_2P_2O_7$ crystallite exposed to reducing conditions, position 4 of the reactor. Note the two sets of shear defects evident along {012} pyro planes due to the loss of lattice oxygen.

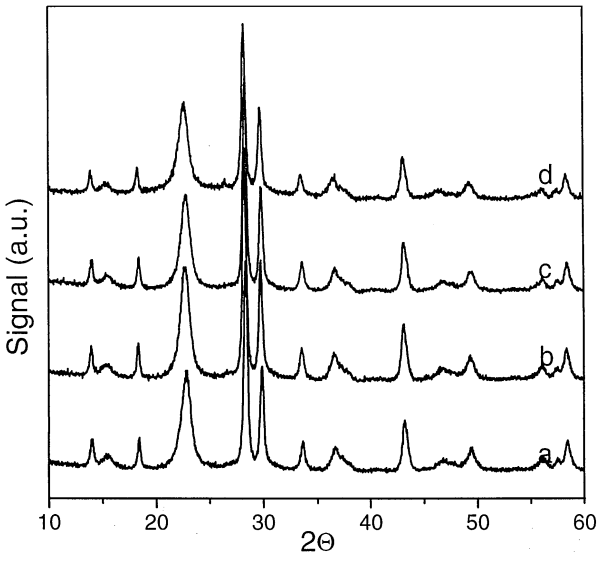

FIG. 7. XRD patterns of catalyst used under oxidizing conditions (curve a) and from positions 1, 2, and 4 of the reactor when a butane-rich feed was employed (curves b, c, and d, respectively).

A theoretical transformation mechanism has also been deduced based on structural modeling studies [8]. The transformation process involves glide/shear defect propagation along the $\langle 012\rangle^{pyro}$ planes, followed by crystallographic shearing in the $\langle 010\rangle$ directions. Similar defects have been noted previously from *in situ* TEM studies of $(VO)_2P_2O_7$ treated under highly reducing atmospheres by Gai and Kourtakis (9).

While XRD measurements were not able to directly identify the formation of either $VOPO_4$ or VPO_4, they were useful for showing the evolution of the pyrophosphate phases along the reactor. Figure 7 displays the XRD patterns for catalyst samples taken from different positions in the reactor used under reducing conditions. Although the $(VO)_2P_2O_7$ reflections are present in all of the samples, it can be seen that the crystallinity decreases slightly along the reactor (see curve d corresponding to position 4 of the reactor), indicating a progressive disorganization of the pyrophosphate phase. On the other hand, the crystallinity of the samples used under oxidizing conditions was high at any position within the reactor: only one set of results (curve a) is shown as a reference in Fig. 7, and it can be seen that the pattern is comparable to that of curve b, which corresponds to material from the reactor entrance under reducing conditions. The decrease of crystallinity with catalyst reduction was confirmed by the evolution of crystal size, calculated from the 200^{pyro} reflection in the XRD pattern as 100, 90, and 79 Å for the samples corresponding to curves b, c, and d of Fig. 7.

The characterization results obtained by different techniques clearly indicate a progressive reduction of the catalyst surface in the reactor used under reducing conditions.

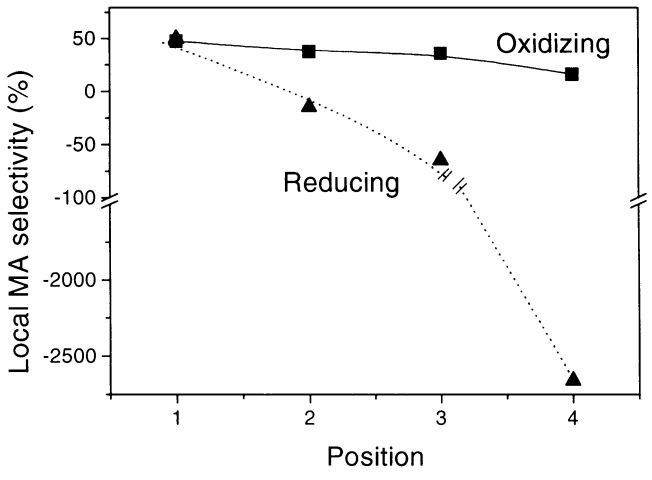

FIG. 8. Variation of the local selectivity with reactor position for catalyst material exposed to oxidizing and reducing conditions.

As shown in Fig. 2, the performance of the catalyst under oxidizing conditions is superior, but this does not show the full difference between butane-rich and oxygen-rich feeds, since most of the reaction in the former case takes place in the first reactor section, where the concentration of oxygen is still relatively high. More illustrative is the plot of the local selectivity to MA, which is defined as the number of moles of MA formed divided by the number of moles of butane reacted *at each of the four reactor sections*. This is shown in Fig. 8 where it can be seen that a dramatic difference exists between the behavior of the catalysts under both sets of conditions. There is a moderate decrease of selectivity along the reactor for the catalyst used under oxygen-rich (oxidizing) conditions as a result of the already-mentioned conversion–selectivity tradeoff in series-parallel reaction networks. With the catalyst used under butane-rich conditions from position 2 onward the local selectivity has negative values, i.e., there is a net destruction of MA. For position 4 the local selectivity reaches values of −1800% which means that there is almost no butane conversion and the scarce oxygen available is being used for MA combustion. It should be noted, however, that the selectivity at the reactor entrance is comparable to that obtained under an oxygen-rich atmosphere. This indicates that the oxygen/butane feed ratio (which has a value of 1.5) in the feed to this reactor section is still sufficient to keep an active and selective catalyst surface.

The above oxygen/butane ratio is probably close to the limit for acceptable performance, as suggested by the results of transient experiments followed by DRIFT. In these experiments the catalyst was first stabilized under a feed containing 2% butane in air (oxygen/butane ratio equal to 10.3), and then the feed composition was shifted to 15% butane in air (oxygen/butane ratio equal to 1.1), while following the changes of the infrared spectra of the catalyst surface. The evolution of the catalyst under reduced conditions (not shown) indicated a strong increase of the main MA bands at 1780 and 1850 cm^{-1}, together with a significant shift of the former toward lower wavenumbers until a new stable state was reached after about 40 min. These results show that, as the catalyst becomes reduced, the concentration of MA on the catalyst surface increases, and its adsorption becomes stronger. Thus, in the reduced catalyst, the strongly adsorbed MA is more likely to react further with any available oxygen, giving deep oxidation products and lowering the MA selectivity.

Operating with a high proportion of butane in the reactor feed may be desirable because of process economics and safety considerations. With the 1–2% butane concentrations currently used in industry, recovery is not economically feasible and unconverted butane is flared. The use of higher concentrations of butane would allow the recycle of unconverted feedstock and reduce the operating costs of the process. It would also allow a safe operation, provided that butane concentrations higher than the upper flammability limit or oxygen concentrations below the minimum oxygen for explosion limit are maintained (10). However, the results presented above indicate that operation in a fixed bed reactor under these conditions would induce detrimental changes on the catalyst surface, leading to the destruction of MA selectivity. Operation with high butane concentrations and good selectivity is still possible, but this requires the use of unconventional contactors, such as circulating fluidized bed reactor systems which have a sufficiently high rate of catalyst transfer between the reactor and the regenerator (11, 12) or membrane reactors where supplementary oxygen is introduced along the bed (13).

CONCLUSIONS

While it is possible to maintain relatively homogeneous catalyst properties in a fixed bed reactor operating with a large excess of oxygen in the feed, when the same reactor was operated under butane-rich conditions very important differences in the state of the catalyst surface became apparent for different reactor positions. The catalyst was progressively reduced along the bed, with the appearance of surface V^{3+} phases for furthermost reactor positions. These changes were found to be detrimental to selectivity: the reduced catalyst became highly unselective, and the available oxygen was used mainly to burn the MA formed near the reactor entrance (where the oxygen/hydrocarbon ratio is more favorable). At the same time, substantial amounts of carbonaceous deposits were formed on the catalyst located toward the exit end of the reactor.

ACKNOWLEDGMENTS

This work was carried out with financial support from the European Commission, Project BRPR-CT95-0046.

REFERENCES

1. Cavani, F., and Trifiró, F., *Catal. Today* **51**, 561 (1999).
2. Centi, G., Fornasari, G., and Trifiró, F., *J. Catal.* **89**, 44 (1984).
3. Ait-Lachgar, K., Tuel, A., Brun, M., Herrmann, J. M., Krafft, J. M., Martin, J. R., Volta, J. C., and Abon, M., *J. Catal.* **177**, 224 (1998).
4. Hutchings, G. J., Desmartin-Chomel, A., Olier, R., and Volta, J. C., *Nature* **368**, 41 (1994).
5. Soejarto, A. D., Coulston, G. W., and Schrader, G. L., *Can. J. Chem. Eng.* **74**, 594 (1996).
6. Rodemerck, U., Kubias, B., Zanthoff, H. W., Wolf, G. U., and Baerns, M., *Appl. Catal.* **153**, 217 (1997).
7. Sajip, S., McPherson, G., Kiely, C. J., Hutchings, G. J., Abon, M., and Volta, J. C., *Proc. ICEM 14* **2**(1), 341 (1998).
8. Sajip, S., Ph.D. thesis, Univ. of Liverpool, Liverpool, UK (1998).
9. Gai, P. L., and Kourtakis, K., *Science* **267**, 661 (1995).
10. Santamaría, J., and Braña, P., "Risk Analysis and Reduction in the Chemical Process Industry," Blackie Academic/Chapman & Hall, Edinburgh, 1997.
11. Contractor, R. M., and Sleight, A. W., *Catal. Today* **3**, 175 (1988).
12. Contractor, R. M., Garnett, D. I., Horowitz, H. S., Bergna, H. E., Patience, G. S., Schwartz, J. T., and Sisler, G. M., *Stud. Surf. Sci. Catal.* **82**, 233 (1994).
13. Mallada, R., Menéndez, M., and Santamaría, J., *Catal Today* **56**, 191 (2000).